Proceedings of the Twenty-fourth (2014) International Ocean and Polar Engineering Conference **www.isope.org**
Busan, Korea, June 15-20, 2014

ISBN 978-1 880653 91-3 (Set); ISSN 1098-6189 (Set)

Numerical Investigation of the Vortex Induced Motion of SPAR in Uniform Current

Weiwen Zhao, Zhirong Shen, Decheng Wan
State Key Laboratory of Ocean Engineering, School of Naval Architecture, Ocean and Civil Engineering,
Shanghai Jiao Tong University, Shanghai, China

ABSTRACT

As the development of model ocean engineering techniques, Spar offshore platforms have been widely used in the area of deepwater drilling. Vortex Induced Motions (VIM), as a common phenomena of Spar platforms exposed to flow, is one of the main factors that affect the lifecycle of offshore platforms and should be avoid as much as possible in the design stage. Two common effective ways to mitigate VIM are the configuration of helical strakes and the adjustment of mooring line stiffness. The former could change the flow pattern in the vicinity of Spar hull and the latter can change the eigenfrequency of platforms in still water to avoid resonance frequency. There have been many investigations on Spar VIM both numerically and experimentally. In this paper, VIM of bared cylinder and straked Spar are compared numerically in uniform current at model scale and at different Reynolds numbers. Fundamental study of VIM is done by comparing motion amplitude at different reduced velocity. To predict the motion of Spar, a spring model is employed. To capture the detailed eddy information of the flow, Large Eddy Simulation (LES) is applied. All the simulation are done at a model scale (1:60).

KEY WORDS: Large Eddy Simulation; Spar; Vortex Induced Motions; OpenFOAM

INTRODUCTION

Spar type offshore platforms are commonly installed in the Gulf of Mexico (GoM). Due to the bluff, vertical columnar hull shape, Spar is subject to VIM when exposed to currents. VIM has a great impact on the lifecycle of Spar platforms, especially the fatigue and wear issues of mooring system.

When vortex sheds at a frequency f_s near eigenfrequency f_0 in still water, the cylinder oscillates violently and the motion amplitude can approach one diameter. Helical strakes were hence designed to reduce the VIM of Spar by interrupt the formulation of vortex near hull.

There have been a lot of publications on Spar VIM in decades. Dijk et al. (2003) did several model tests in MARIN. The objective is to evaluate the Vortex Induced Vibration (VIV) response of truss Spars and to optimize their strake configurations. Smith et al. (2004) studied the effects of loop / eddy current on Spar VIM and the fatigue and wear issues for mooring systems of Spars subject to VIM. Halkyard et al. (2005) made a benchmarking of Truss Spar VIM with CFD and experiments. The focus was on the effect of current direction, reduced velocity and strake pitch on the VIM response. The works were done using a finite element code AcuSolve. Atluri et al. (2006) simulated a Truss Spar model at model scale 1:40 which was focus on the hydrodynamic effects on Spar VIM introduced by holes on strakes and hull apendage. Their works were also done with AcuSolve. Sirnivas et al. (2006) applied a new generation of LES type model for the simulation of flow around a Spar hull. This new method involved a Variational Multiscale formulation, allowing etter capture of the back scatter. And the simulation was compared with experimental data from a model test. Finnigan and Roddier (2007) did some model tests at Super Critical Reynolds Numbers. The effects of appurtenances and current heading on strake effectiveness and VIM response were discussed. Oakley Jr. and Constantinides (2007) tested a newly developed meshing techniques and seeking an understanding of how spar appurtenances interact. The model have a high fidelity, and many details like strakes, pipes, chains and anodes were included.

The existence of strakes and more complex geometry such as appurtenances are the main reason that there are curently no effective analytical method for predicting Spar VIM. This paper aims at the initial strakes design for Spar platform, and testing the capability of CFD working condition in predicting Spar VIM.

There were also several numerical investigation of flow over a cylinder or cylinders. Liang and Wan (2009) had some numerical investigations of cylinder transversely forced oscillation in uniform current with low Reynolds number at 200. The work was focused on the hydrodynamic forces on the cylinder, as well as the wake pattern change of vortex shedding. Cao and Wan (2010) studied the numerical simulation of the flows aroundsingle and two circular cylinders in tandem arragement by OpenFOAM solver. The Reynolds numbers were at a range of 100-300. Duan and Wan (2013) studied a three-dimensional simulation of flow around a cylinder at Reynolds number of 3900. The works were done by applying LES turbulence approaches provided by OpenFOAM solvers. The numerical results showed good agreement with the experimental ones.

In this paper, we present two models to study the fundamental

phenomenon of Spar VIM and the reduction of VIM, by using numerical techniques of Computational Fluid Dynamics (CFD). The investigation was achieved by the open source CFD toolbox OpenFOAM. All the simulation are performed by solving the incompressible Navier-Stokes equation using the LES model and Smagorinsky sub-grid scale model. The PISO algorithm, proposed by Issa (1986) for the velocity-pressure decoupling, is used for solving the coupled velocity and pressure.

NOMENCLATURE

A	Dynamic oscillation amplitude	(m)
B	Linear damping of spring	(kg/s)
D	Diameter of cylinder or spar hull	(m)
f_0	Eigenfrequency in still water	(Hz)
f_s	Vortex shedding frequency	(Hz)
H	Draft of Spar hull	(m)
K	Spring stiffness	(N/m)
L	Total length of Spar hull	(m)
M	Mass of cylinder or spar hull	(kg)
U	Current velocity or towing velocity	(m/s)
$U_{rn} = \frac{U}{f_0 D}$	Reduced velocity	(-)
$St = \frac{f_s D}{U}$	Strouhal number	(-)
$Re = \frac{UD}{\nu}$	Reynolds number	(-)

TURBULENCE MODEL

Due to the limitation of the computer resources, the Direct Numerical Simulation (DNS) is not feasible for engineering problems which mostly are at high Reynolds numbers. While statistical turbulence models such as Reynolds-Averaged Navier-Stokes (RANS) and Unsteady RANS (URANS) poorly predict the overall flow as the insufficient capture of eddy information. We consider Large Eddy Simulation (LES) suitable for our simulation.

In LES model, the instantaneous velocity field U_i is divided into two parts: a large scale local averaged part $\overline{u}_i$ which is directly calculated, a sub-grid scale part $\overline{u}_i'$ which should be modeled using Sub-Grid Scale (SGS) models. The filtered velocity is defined by:

$$\overline{u}_i(x) = \int G(x, x')u_i(x')\mathrm{d}x', \tag{1}$$

where $G(x, x')$, which is called the filter kernel, is a localized function. The Navier-Stokes equation of incompressible flow after applying filter kernel can be expressed as follows:

$$\frac{\partial(\rho\overline{u}_i)}{\partial t} + \frac{\partial(\rho\overline{u_i u_j})}{\partial x_j} = -\frac{\partial \overline{p}}{\partial x_i} + \frac{\partial}{\partial x_j}\left[\mu\left(\frac{\partial \overline{u}_i}{\partial x_j} + \frac{\partial \overline{u}_j}{\partial x_i}\right)\right], \tag{2}$$

$$\frac{\partial \overline{u}_i}{\partial x_i} = 0. \tag{3}$$

Here the subgrid scale Reynolds stress τ_{ij} is introduced, and defined as follows:

$$\tau_{ij} = -\rho(\overline{u_i u_j} - \overline{u}_i\overline{u}_j). \tag{4}$$

The most commonly used subgrid scale model Smagorinsky is chosen for turbulence closure:

$$\tau_{ij} - \frac{1}{3}\tau_{kk}\delta_{ij} = 2\mu_t\overline{S}_{ij}, \tag{5}$$

where μ_t the eddy viscosity and $\overline{S}_{ij}$ the strain rate of the large scale. The form of the subgrid scale eddy viscosity is:

$$\mu_t = C_S^2\rho\Delta^2\left|\overline{S}\right|, \tag{6}$$

where $\left|\overline{S}\right| = \sqrt{2\overline{S}_{ij}\overline{S}_{ij}}$ and the stress rate is defined as

$$\overline{S}_{ij} = \frac{1}{2}\left(\frac{\partial \overline{u}_i}{\partial x_j} + \frac{\partial \overline{u}_j}{\partial x_i}\right), \tag{7}$$

and Δ denotes the filter length scale, $\Delta = (\Delta_x\Delta_y\Delta_z)^{1/3}$.

The finite volume method (FVM) is used for spatial discretization and implicit Euler scheme is used for temporal discretization. For the solution of coupled pressure and velocity, the PISO (pressure implicit with splitting of operator) algorithm (Issa, 1986) is applied. This algorithm uses one predictor step and two corrector steps to solve the Navier-Stokes equations.

6DoF MODEL

The 6DoF motion solver been employed here was firstly used by Shen and Wan (2011, 2012). Two right-handed coordinate system are introduced, one is the earth-fixed coordinate system, and the other is rigid body fixed coordinate system. The two coordinate system are couple with each other by the *Euler angles* of the rigid body. More details about the 6DoF model can be found in references (Carrica et al., 2007).

DYNAMIC MESH DEFORMATION

To simulate the movement of rigid body, the dynamic mesh deformation techniques is applied. Cells will translate, stretch and deform during computing, while the topological relationships of mesh remain unchanged. The *r*-method (Cai et al., 2004) is a dynamic grid deformation method without changing the topological relationships of meshes. In contrast with local based method, the velocity based type of grid method is chosen for its simplicity and effectiveness. Readers can refer to reference (Wan, 2008) for more details.

GEOMETRY AND CONDITIONS

The geometry as well as other important properties of two models are described in this section. The Spar model chosen in this study is at a model scale $\lambda = 1:60$ and the diameter D of the Spar hull is 0.568m. The draft H and total length L of Spar hull are 3.302m and 3.582m respectively. The Spar has 3 helical strakes with a width of $13\%D$ and a pitch of $2.7D$. The bare cylinder geometry is the same as the Spar hull, but without helical strakes. And the total displacement is 808.32 kg. The model of bare cylinder and Spar model are shown in Fig. 1(a) and Fig. 1(b) respectively.

Previous study by Halkyard et al. (2005) shows the reduced velocity is appoximate $U_{rn} = 6 \sim 8$ in VIM lock-in range. The simulation conditions in this study are bare cylinder and straked Spar model at different flow velocity. Three velocities case which are in lock-in range are chosen so that cylinder oscillating at a large scale. The reduced velocities U_{rn} of three cases are 6, 7 and 8, with corresponding to real flow velocities 0.36, 0.42 and 0.48 m/s respectively.

To predict Spar VIM, a spring model is employed. Since surge and sway are the dominant motions in VIM, our model is constrained in this two

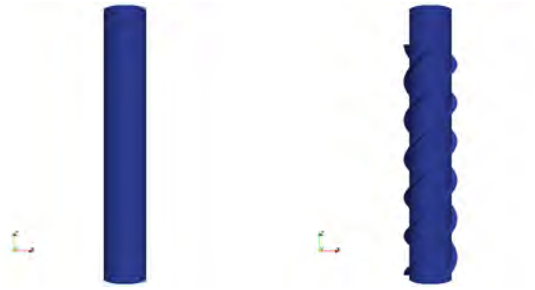

(a) Bare cylinder (b) Straked Spar

Fig. 1: Geometry of bare cylinder and Spar model

degrees of freedom by been held in place with two springs, which are arranged in in-line and cross-flow direction respectively. The linear spring stiffness K is 725 N/m. A sketch of spring model is show in Fig. 2.

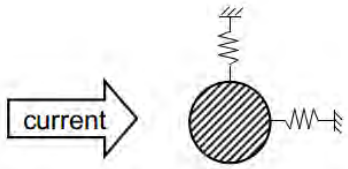

Fig. 2: Sketch of spring model

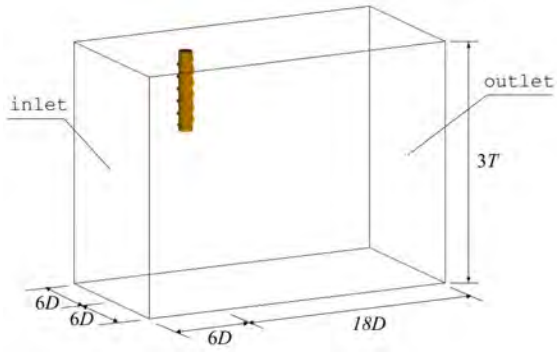

Fig. 3: Computational domain

The movements of the hull are limited in a horizontal plane, thus the motion equations for the hull body are expressed as:

$$M\ddot{x} + B\dot{x} + Kx = F_{hx}, \tag{8a}$$

$$M\ddot{y} + B\dot{y} + Ky = F_{hy}, \tag{8b}$$

where subscript hx and hy denote the components of hydrodynamic forces at in-line and cross flow directions, respectively. Fig. 3 shows the computational domain which are used in this study. Its geometry is defined as follows, the length (x-direction) is $24D$ and the width (y-direction) is $12D$. The height is $3H$ in order to avoid shallow water effects. The upstream boundary is a simple velocity inlet condition of the current velocity. The downstream boundary is a pressure outlet condition in which the integral of pressure equals to 0. The top and two sides of the domain is symmetry, and bottom is a free-slip boundary condition.

Table 1: Case conditions

Case No.	Reduced velocity	Flow velocity (m/s)	Reynolds number
1	6	0.36	2.04e5
2	7	0.42	2.39e5
3	8	0.48	2.73e5

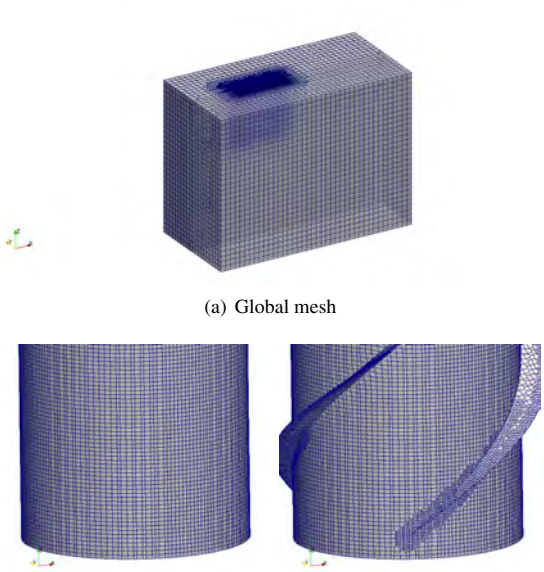

(a) Global mesh

(b) Local mesh (bare cylinder) (c) Local mesh (straked Spar)

Fig. 4: Computational mesh

`SnappyHexMesh` is a mesh generation utility supplied with OpenFOAM. It can generate unstructured meshes containing hexahedra (hex) and split-hexahedra (split-hex) automatically. To capture the details of wake eddy of VIM, the downstream vortex shedding region should be refined to ensure the grid is small enough to capture small scale of eddies. There are three types of mesh refinement in `SnappyHexMesh`, feature edge refinement, surface refinement and region refinement. `SnappyHexMesh` firstly extract feature edges and surfaces from 3D CAD model files such as STL, NAS files. Those edges and surfaces are then refined at different user-specified levels in `snappyHexMeshDict` file. The user-specified regions are also refined at its own refinement levels.

`SnappyHexMesh` refines mesh by iteratively splitting cells into small ones and morphing the resulting split-hex mesh to the surface. The refinement iteration initially starts with backgroud mesh which is usually a simple and orthogonal mesh. In our case, a 3-level refinement box region which wraps the Spar hull is applied, as shown in Fig. 4. The strakes surface and feature edge are refined at level 5 and 6 respectively. The total cells of the computational domain for bare cylinder and straked Spar model are 2,950,000 and 3,090,000 respectively.

The simulation is running on a Linux cluster named "PI" at the Shanghai Jiao Tong University High Performance Computing Center (SJTU HPCC). Each node of "PI" has two Intel Xeon E5-2670 CPUs (8 Cores, 2.6GHz) and 64GB memory. All nodes are connected with each other using the InfiniBand cables for high-speed data exchange. Running with 2 nodes or 32 CPU cores, it takes about 48 hours to simulate 150s with a time step of 0.02s.

RESULTS

There are several measures to evaluate Spar VIM. The amplitude over diameter y/D was carried out first for its intuitive. Soon people realized its not suitable to describe motions using time series of motion amplitude. And the so-called "average maximum" , "nominal maximum" and "stanard deviation" response were proposed. The "average maximum" is defined as $A_{ave} = (\mathrm{MAX}(y/D) - \mathrm{MIN}(y/D))/2$, and "nominal maximum" is defined as $A^* = \sqrt{2}\mathrm{RMS}(y/D)$. Atluri et al. (2006) suggested that the stanard deviation is a better measure for comparison rather than average maximum as the latter depends greatly on the time length of simulation. In this study, we give the raw sway amplitude time series of VIM in order to compared the maximum sway more intuitively. The VIM motion trajectories are given in Fig. 5, the blue dotted line represent the trajectory of bare cylinder without strakes, and the red real line represent the trajectory of the straked Spar model. Take a close look at Fig. 5(c), which the reduced velocity is $U_{rn} = 8$. The VIM response of bare cylinder shapes a twisted "8", while the response of straked Spar model looks like a "banana". The bare cylinder oscillates at a amplitude nearly equal to D in both in-line and cross flow directions. Strakes have a good effect on reducing VIM response in both in-line (x-direction) and cross flow (y-direction). Especially in cross flow direction, the surge of straked Spar changes at a small scale, while the transverse sway is the dominant motion which oscillates at a amplitude of $0.5D$.

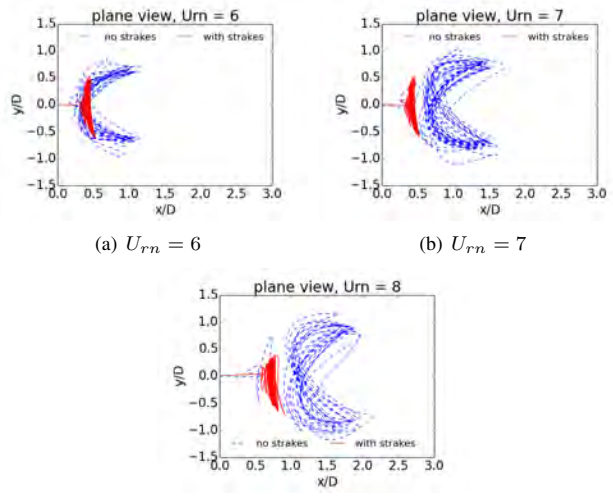

(a) $U_{rn} = 6$ (b) $U_{rn} = 7$

(c) $U_{rn} = 8$

Fig. 5: Plane view of trajectory

The time series of transverse motion amplitude are shown in Fig. 6. Both bare cylinder and Spar hull oscillate periodically and regularly. Bare cylinder oscillates transversely at a larger amplitude than straked Spar, especially at $U_{rn} = 8$.

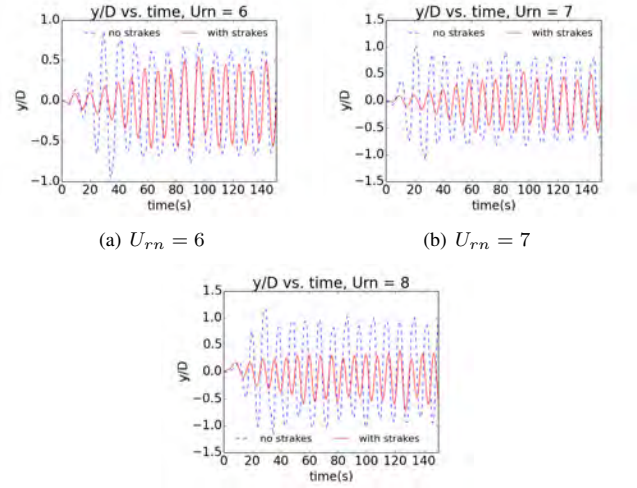

(a) $U_{rn} = 6$ (b) $U_{rn} = 7$

(c) $U_{rn} = 8$

Fig. 6: Time series of cross flow motion amplitude

Fig. 7 shows the time histories of total forces on two models. The forces here contain linear spring forces and hydrodynamic forces. Take a look at these figures, the force of bare cylinder changes at a large scale compared to the straked one due to the linear spring forces caused by the large motion amplitudes.

Fig. 8 is isosuface contour of the the second invariant of the velocity gradient tensor Q (Hunt et al., 1988) colored with x-direction velocity component. The flow seperation and wake pattern are observed from the figures. Fig. 8(a) and Fig. 8(c) show the bare cylinder and straked Spar at a maximum sway offset, and Fig. 8(b) and Fig. 8(d) are at a negative maximum sway offset. The differences of wake patterns and flow seperation points are evident for two models. In the case of bare cylinder, when cylinder hull at a maximum offset, most of vortices shed from the other side, which yields vortex shedding forces become extra large. While for the straked Spar, most flow seperation points are on strakes. The existence of strakes impedes the formation of large vortices and breaks the regular vortex shedding process to mitigate VIM response. Fig. 9 clearly shows the streamlines being diverted by strakes. This may help better understanding the behavior of strakes and provide information for design of strakes configurations.

CONCLUSION

In this study, a bare cylinder and a Spar model with 3 strakes are choosen to estimate the VIM mitigation of helical strakes. We present the numerical simulation on these two models at reduced velocities $U_{rn} = 6, 7, 8$ using a modified `pimpleDyMFoam` solver from the open source CFD toolbox OpenFOAM. Based on the stock single phase incompressible Navier-Stokes solver `pimpleDyMFoam`, we developed a six-degrees-of-freedom (6DoF) motion model, and a linear spring model for the Spar VIM numerical simulation. The motion of Spar is constrained in horizontal plane, thus Spar can only have surge and sway displacements. Detailed structures of flow field in the vicinity of hull are obtained by applying the instantaneous turbulence approaching model LES. Flow seperation, vortex shedding, wake pattern are observed, and oscillating amplitude and period are analyzed. The vortex shedding

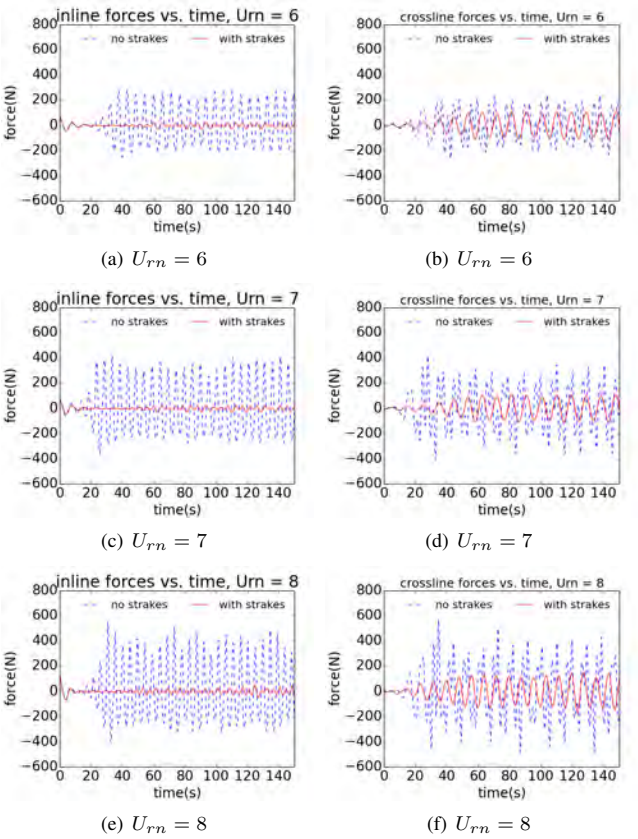

(a) $U_{rn} = 6$ (b) $U_{rn} = 6$

(c) $U_{rn} = 7$ (d) $U_{rn} = 7$

(e) $U_{rn} = 8$ (f) $U_{rn} = 8$

Fig. 7: Time series of in-line forces

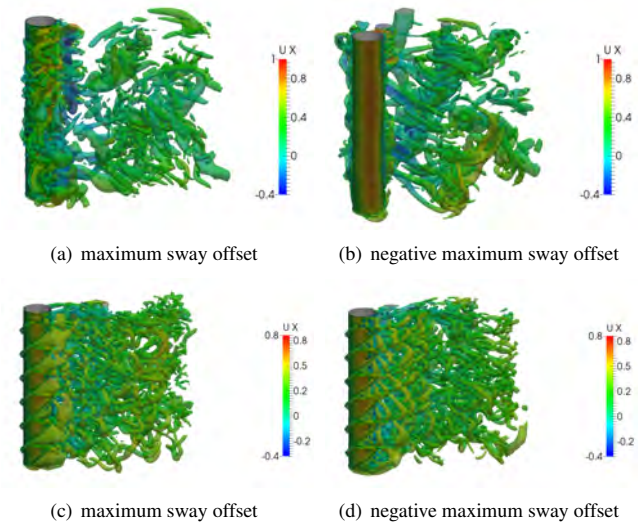

(a) maximum sway offset (b) negative maximum sway offset

(c) maximum sway offset (d) negative maximum sway offset

Fig. 8: Vorticity contour at $U_{rn} = 7$

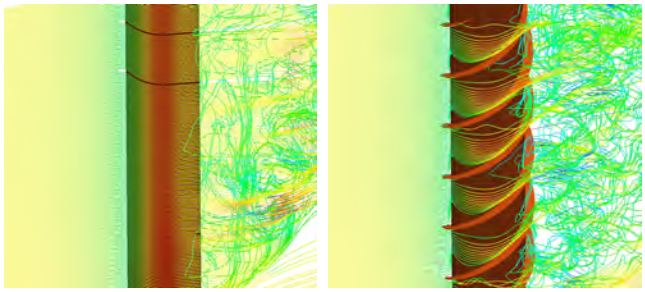

(a) Bare cylinder (b) Straked Spar

Fig. 9: Streamwise at $U_{rn} = 7$

regime are studied carefully, and the lock-in range is successfully simulated. The numerical results show that strakes have a good effect on the mitigation of Spar VIM.

However, there are some issues remain to be resolved in our future work. The first rised important one is the validation of CFD for predicting Spar VIM. All these numerical simulations in this paper should have mesh convergence validation been done and be further compared with tow tank or circulation water basin experiments. Next is the influences of turbulence models on Spar VIM. Although we've accomplished the comparison of RANS and LES in our previous work, the results which are not given in this paper show that LES successfully captures the main feature of flow patterns in three-dimensional effect, while RANS did not. The Detached Eddy Simulations (DES) is considered a more prospective turbulence model in contrast with LES as it can applying wall functions near walls and reduce mesh economy.

ACKNOWLEDGEMENT

This work is supported by National Natural Science Foundation of China (Grant No. 11072154, 51379125), The National Key Basic Research Development Plan (973 Plan) Project of China (Grant No. 2013CB036103), High Technology of Marine Research Project of The Ministry of Industry and Information Technology of China, the Program for Professor of Special Appointment (Eastern Scholar) at Shanghai Institutions of Higher Learning, and Center for HPC of Shanghai Jiao Tong University, to which the authors are most grateful.

REFERENCES

Atluri, S., Halkyard, J., and Sirnivas, S. (2006). "CFD simulation of Truss Spar Vortex-Induced Motion." In *Proceedings of the International Conference on Offshore Mechanics and Arctic Engineering - OMAE*, Vol. 2006.

Cai, X.-X., Jiang, B., and Liao, G. (2004). "Adaptive grid generation based on the least-squares finite-element method." *Computers & Mathematics with Applications*, Vol. 48, No. 78, pp. 1077–1085.

Cao, H. and Wan, D. (2010). "Application of OpenFOAM to simulate three-dimensional flows past a single and two tandem circular cylinders." In *Proceedings of the International Offshore and Polar Engineering Conference*, Vol. 3, pp. 702–709.

Carrica, P. M., Wilson, R. V., Noack, R. W., and Stern, F. (2007). "Ship motions using single-phase level set with dynamic overset grids." *Computers & Fluids*, Vol. 36, No. 9, pp. 1415–1433.

Dijk, R., Magee, A., Perryman, S., and Gebara, J. (2003). "Model Test

Experience on Vortex Induced Vibrations of Truss Spars." The Offshore Technology Conference.

Duan, M. and Wan, D. (2013). "Large eddy simulations of flow around a 3D cylinder at subcritical reynolds number." In *Proceedings of the International Offshore and Polar Engineering Conference*, Anchorage, ISOPE, Vol 3, pp. 372–378.

Finnigan, T. and Roddier, D. (2007). "Spar VIM model tests at supercritical reynolds numbers." In *Proceedings of the International Conference on Offshore Mechanics and Arctic Engineering* - ASME Vol. 3, pp. 731–740.

Halkyard, J., Sirnivas, S., Holmes, S., Constantinides, Y., Oakley, O., and Thiagarajan, K. (2005). "Benchmarking of truss spar vortex induced motions derived from CFD with experiments." In *Proceedings of the International Conference on Offshore Mechanics and Arctic Engineering - ASME*, Vol. 3, pp. 895–902.

Hunt, J. C., Wray, A., and Moin, P. (1988). "Eddies, streams, and convergence zones in turbulent flows." In *Studying Turbulence Using Numerical Simulation Databases, 2*, Vol. 1, pp. 193–208.

Issa, R. I. (1986). "Solution of the implicitly discretised fluid flow equations by operator-splitting." *Journal of Computational physics*, Vol. 62, No. 1, pp. 40–65.

Liang, L. and Wan, D. (2009). "Numerical investigation of a forced oscillating cylinder in a cross flows with low Reynolds number." *China Ocean Engineering*, No. 04, pp. 45–53+60.

Oakley Jr., O. and Constantinides, Y. (2007). "CFD truss spar hull benchmarking study." In *Proceedings of the International Conference on Offshore Mechanics and Arctic Engineering - ASME*, Vol. 3, pp. 703–713.

Shen, Z. and Wan, D. (2011). "Numerical simulation of sphere water entry problem based on VOF and dynamic mesh methods." In *Proceedings of the International Offshore and Polar Engineering Conference*, Maui, Hawaii, ISOPE, Vol 3, pp. 695–702.

Shen, Z. and Wan, D. (2012). "Rans computations of added resistance and motions of ship in head waves." In *Proceedings of the Int-Offshore and Polar Eng Conf*, Rhodes, ISOPE, V3, pp. 1096–1103.

Sirnivas, S., Allain, O., Wornom, S., Dervieux, A., and Koobus, (2006). "A study of LES models for the simulation of a turbulent flow around a truss Spar geometry." In *Proceedings of the International Conference on Offshore Mechanics and Arctic Engineering - ASME*, Vol. 2006.

Smith, D., Kokkinis, T., Thompson, H., and Greiner, W. (2004). "Hindcasting VIM-induced mooring fatigue for the Genesis spar." In *Proceedings of the International Conference on Offshore Mechanics and Arctic Engineering - ASME*, Vol. 1 B, pp. 1005–1014.

Wan, D. (2008). "Grid deformation-multigrid fictitious boundary method for cylinder undergoing vortex-induced motions." In *Proceedings of the International Offshore and Polar Engineering Conference*, Vancouver, BC, Canada, ISOPE, Vol 3, pp. 24–31.